Bioinformatics, 32(11), 2016, 1670–1677
doi: 10.1093/bioinformatics/btw217
Advance Access Publication Date: 28 April 2016
Original Paper

OXFORD

Sequence analysis

Informed *k*mer selection for *de novo* transcriptome assembly

Dilip A. Durai[1,2] and Marcel H. Schulz[1,2,*]

[1]Cluster of Excellence on Multimodal Computing and Interaction, Saarland University, Saarbrücken, 66123, Germany and [2]Department for Computational Biology and Applied Algorithmics, Max Planck Institute for Informatics, Saarbrücken, 66123, Germany

*To whom correspondence should be addressed.
Associate Editor: Gunar Ratsch

Received on April 7, 2015; revised on December 31, 2015; accepted on April 17, 2016

Abstract

Motivation: *De novo* transcriptome assembly is an integral part for many RNA-seq workflows. Common applications include sequencing of non-model organisms, cancer or meta transcriptomes. Most *de novo* transcriptome assemblers use the de Bruijn graph (DBG) as the underlying data structure. The quality of the assemblies produced by such assemblers is highly influenced by the exact word length *k*. As such no single *k*mer value leads to optimal results. Instead, DBGs over different *k*mer values are built and the assemblies are merged to improve sensitivity. However, no studies have investigated thoroughly the problem of automatically learning at which *k*mer value to stop the assembly. Instead a suboptimal selection of *k*mer values is often used in practice.
Results: Here we investigate the contribution of a single *k*mer value in a multi-*k*mer based assembly approach. We find that a comparative clustering of related assemblies can be used to estimate the importance of an additional *k*mer assembly. Using a model fit based algorithm we predict the *k*mer value at which no further assemblies are necessary. Our approach is tested with different *de novo* assemblers for datasets with different coverage values and read lengths. Further, we suggest a simple post processing step that significantly improves the quality of multi-*k*mer assemblies.
Conclusion: We provide an automatic method for limiting the number of *k*mer values without a significant loss in assembly quality but with savings in assembly time. This is a step forward to making multi-*k*mer methods more reliable and easier to use.
Availability and Implementation:A general implementation of our approach can be found under: https://github.com/SchulzLab/KREATION.
Supplementary information: Supplementary data are available at *Bioinformatics* online.
Contact: mschulz@mmci.uni-saarland.de

1 Introduction

With the massive amounts of RNA-seq data (Sultan *et al.*, 2008) produced for many non-model organisms, the interest for *de novo* analyses of RNA-seq data has increased over the last few years. These analyses include the *de novo* assembly of full length transcripts, expression level computation of novel transcripts, detecting differentially expressed transcripts and detection of related genes in close species or polymorphism detection (Davidson and Oshlack, 2014; Haznedaroglu *et al.*, 2012; Le *et al.*, 2013; Sloan *et al.*, 2012).

Due to the large number of applications, several methods have been proposed for the *de novo* transcriptome assembly. Most of these methods are based on building a de Bruijn graph (DBG) from the RNA-seq reads. The nodes of the DBG are substring of length *k* (also know as *k*mers) obtained from the reads and two nodes are connected if they have *k*-1 overlap. After obtaining the DBG, various heuristic algorithms are used to predict alternative transcripts from each DBG component. These algorithms either use a single *k*mer value (Chang *et al.*, 2015; Grabherr *et al.*, 2011; Xie *et al.*,

2014) or merge transcripts generated from multiple *k*mer values to obtain a final non-redundant assembly (Peng *et al.*, 2013; Robertson *et al.*, 2010; Schulz *et al.*, 2012; Surget-Groba and Montoya-Burgos, 2010). A multi-*k*mer based approach outperforms a single-*k*mer based approach as one *k*mer size rarely fits all genes (Chang *et al.*, 2015; Peng *et al.*, 2013; Schulz *et al.*, 2012). Large kmer values resolve repeats and regions with many errors, whereas small *k*mer values are necessary to connect lowly expressed transcripts that have low-coverage regions. Hence even for most single *k*mer methods it is beneficial to run the assembler for different *k*mer values and merge the final results.

But the question about the core set of *k*mer sizes that are needed to achieve a good quality assembly has received little attention for multi-*k*mer methods. Currently, approaches (i) use the default *k*mer series of the assembler which is tuned on a limited number of datasets, (ii) select an arbitrary subset of *k*mer sizes or (iii) use all possible *k*mer sizes for the assembly. In practice that means that most often the resulting assembly is suboptimal. Either important *k*mer sizes are missed (cases 1–2) and therefore the sensitivity is reduced or the complete assembly contains more misassemblies than necessary and has wasted computational resources (case 3).

Selecting a suitable *k*mer size for *de novo* assembly has been previously explored in the context of genomic sequencing. For example (Chikhi and Medvedev, 2014) devised a method to select the best *k*mer size for *de novo* genome assembly. Simpson devised a method to estimate a number of interesting characteristics like paths with variations or repeats in the DBG for different *k*mer sizes from a FM-index over the reads (Simpson, 2014). Further, computing an optimal *k*mer range for *de novo* read error correction was also proposed (Ilie *et al.*, 2011, Schulz *et al.*, 2014). However, all these methods assume a uniform coverage distribution and are not applicable to non-uniform RNA-seq data.

Here we investigate in detail how the number of *k*mer assemblies can be minimized to save computational resources, without a large loss in sensitivity and without using a reference annotation for assembly quality assessment. We introduce the KREATION (Kmer Range EstimATION) algorithm that is based on two novel contributions: (i) a comparative clustering of single *k*mer assemblies to define *extended clusters* which gives a notion of the assembly quality and (ii) a heuristic model assessment that allows to predict the optimal stopping point for a multi-*k*mer assembly method. We show that our new *de novo* strategy automates the choice of *k*mer sizes to explore, while achieving close to optimal performance.

2 Methods

2.1 Evaluation of assemblies

We use standard metrics for the evaluation of our assembled transcripts. We align transcripts against the reference genome using Blat (Kent, 2002,version 36) and compare it with annotated Ensembl transcripts (Cunningham *et al.*, 2014,version 65). Then we compute the number of Ensembl transcripts that are overlapped to at least 80 or 100% by an assembled transcript, and term them as *80* and *100%-hits*, respectively. We defined *80%-hit improvement rate* as the ratio of the 80%-hits obtained from the multi-*k*mer assembly compared to a single-*k*mer based assembly. Further, we compute *misassemblies* by counting the number of aligned transcripts whose aligned region is $\leq 95\%$ of the total transcript length. All transcripts that are not misassemblies are considered to be *correct*. We also compute nucleotide sensitivity and specificity as explained by (Schulz *et al.*, 2012).

2.2 Transcriptome assembly

We used the *de novo* transcriptome assemblers Oases (Schulz *et al.*, 2012, version 0.2.08), SOAPdenovo-Trans (Xie *et al.*, 2014, version 1.03) and Trans-ABySS (Robertson *et al.*, 2010 version 1.5.3) for our analyses. All assemblers were run with default parameters except the *k*mer parameter for the DBG and insert length for the paired-end sequencing data sets. Transcripts shorter than 100bps were removed from the final assembly.

SOAPdenovo-Trans doesn't have its own merge script and the merge script of Oases and TransABySS provides little information about the clusters obtained. Further, it was shown that the oases_merge script has suboptimal performance compared to CD-HIT-EST clustering (Haznedaroglu *et al.*, 2012). Hence we used CD-HIT-EST (Fu *et al.*, 2012, version 4.6.1-2012-08-07) for clustering individual *k*mer assemblies, as detailed in Section 2.3.

In order to analyze how selecting arbitrary *k*mer values influences assembly performance we created three sets of *random k*mers. All the sets contained *k*mers spread across the read length, see Table 1.

We denote as *best-k* the assembly where the highest number 80%-hits was achieved for a dataset. For the analyzed datasets these were assemblies obtained from $k=25$ for brain, $k=23$ for human Embryonic Stem Cell (hESC), $k=27$ for T-cell and HeLa.

2.3 Clustering assembled transcripts

We use the CD-HIT-EST software, for clustering transcripts assembled by individual *k*mer sizes and merging sets of transcripts from distinct *k*mers. CD-HIT-EST is a fast clustering technique that reports final clusters with all sequences contained in the cluster. It uses a greedy algorithm to iteratively grow clusters and multicore parallelization for fast clustering. We run CD-HIT-EST with 10 threads.

Consider two sets of assembled transcripts, $\mathcal{T}_1 = \{t_1^1, \ldots, t_n^1\}$ and $\mathcal{T}_2 = \{t_1^2, \ldots, t_m^2\}$ with n and m many sequences respectively, each produced by running a *de novo* assembler for one or more *k*mer values. Let $\mathcal{C} = \{c_1, \ldots, c_l\}$ be the set of l sequence clusters obtained by applying a sequence clustering algorithm to $\mathcal{T}_1$ and $\mathcal{T}_2$, denoted as $ComputeClusters(\mathcal{T}_1, \mathcal{T}_2)$. We define the following notions on clusters: a cluster $c \in \mathcal{C}$ is called *unique* with respect to $\mathcal{T}_2$ if it holds that $c \subset \mathcal{T}_2$, namely that all sequences in c are only from assembly $\mathcal{T}_2$. Further we call the longest sequence of a cluster $c \in \mathcal{C}$ the *representative* of c, denoted as $rep(c)$. A cluster $c \in \mathcal{C}$ is called *extended* by $\mathcal{T}_2$ if $\text{rep}(c) \in \mathcal{T}_2$ and c is not unique. We denote $e = \text{extended}(\mathcal{C}, \mathcal{T}_2)$ as the number of extended clusters in $\mathcal{C}$ with respect to $\mathcal{T}_2$ (See Supplementary Figure S1). Collectively we denote all clusters that are extended or unique with respect to $\mathcal{T}_2$ as *novel* clusters with respect to $\mathcal{T}_2$. All remaining cluster are called *old*.

2.4 Predicting the assembly stopping point via assessment of model fit

We analyzed assemblies generated by different de novo assemblers and observed that with an increase in *k*mer size the number of

Table 1. Sets of random *k*mer values used to analyze the effect of selecting arbitrary *k*mer values on the assembly. Rows represents the sets and columns represent the dataset with read length mentioned in brackets

	Brain (50)	TCell (45)	hESC (50)	HeLa (76)
Set1	25,33,37,45	25,33,37,45	25,33,37,45	25,39,53,61
Set2	25,31,35,43	25,31,35,43	25,31,35,43	35,43,57,69
Set3	23,33,37,45	23,33,37,45	23,33,37,45	51,55,69,71

correct transcripts produced by the assembler follows approximately an exponential distribution, see Results. We show that the number of extended clusters in consecutive assemblies behave similarly and can thus be used in a *de novo* setup. Our rationale was that once this exponential trend does not hold anymore for increasing *k*mer values, the number of extended clusters is not dominated by correct transcripts, but rather by missassemblies or redundant assemblies.

We summarize our approach for the above insight in algorithm 1: Given a set of reads and a minimal *k*mer, denoted $k_{\min}$, the assembler explores an *a priori* fixed series of *k*mer values $\mathbf{X} = (k_1, \ldots, k_n)$ where $k_1 = k_{\min}$. This series is computed using a function *f*. In our case we use the simple function: $f(k) = k + 2$, as Oases and SOAPdenovo-Trans can use odd *k*mer values only and we wanted to use the same set of *k*mer values for all assemblers to maintain consistency. For each k an assembly is produced (line 7). All new transcripts in $\mathcal{T}_{k_i}$ are clustered with the previous transcripts using the function $ComputeClusters(\mathcal{T}, \mathcal{T}_{k_i})$ to produce $\mathcal{C}$ (line 8). The number of extended clusters e_i with respect to $\mathcal{T}_{k_i}$ is computed (using $extended(\mathcal{C}, \mathcal{T}_{k_i})$) and its log count is stored in y_i (line 9).

We then assume the following linear model:

$$\mathbf{Y} = \beta_0 + \beta_1 \ \mathbf{X} + \epsilon\,, \tag{1}$$

where $\mathbf{Y} = (y_1, y_2, \ldots, y_n)$ denotes the series, with $y_i = \log_{10}(e_i)$. β_0 and β_1 are the constants representing *slope* and *intercept* of the line respectively. Gaussian noise is denoted by ϵ.

We are interested in analyzing the linear model fit with an increase in number of data points. More precisely, if we have a linear model fit on $n-1$ datapoints (where $n > 3$, since we require at least three datapoints to model a line to avoid premature stopping of the assembly), we want to assess the error in predicting the nth datapoint using the line. We fit a line (*lm*) with $\mathbf{Y} = (y_1, y_2, \ldots, y_{n-1})$ and $\mathbf{X} = (k_1, k_2, \ldots, k_{n-1})$ and estimate the coefficients $\widehat{\beta}_{n-1} = (\beta_0, \beta_1)$ by minimizing the residual sum of squares (line 10):

$$\widehat{\beta}_{n-1} = \arg\min_{\beta} \sum_{i=1}^{n-1} (y_i - \widehat{y}_i)^2\,, \tag{2}$$

where $\widehat{y}_i = \beta_0 + \beta_1 \ k_i$ is the predicted value of y_i. Assuming that this line would also explain y_n, we use the estimated coefficients to compute $\widehat{y}_n$ for k_n (line 11). We compute the error between $\widehat{y}_n$ and its actual value:

$$\mathrm{err}(n) = (y_n - \widehat{y}_n)^2\,. \tag{3}$$

We increment n and repeat the above procedure until n reaches the stopping point. For any given *k*mer series of length m, we define the *deviation score (d_score)* as the cumulative sum of point-wise error estimates:

$$d\_score_m = \sum_{n=4}^{m} \mathrm{err}(n)\,. \tag{4}$$

The stopping point is determined by applying a threshold to the *d_score* (line 13). The *d_score* is expected to remain close to zero for data points which follow a linear trend. It increases considerably and crosses the threshold value at a point where the quality of the linear fit degrades i.e. the fitted line is no longer able to explain the additional datapoint. If the *d_score* is less than the cutoff, the algorithm continues and updates all the variables (line 16–18). Otherwise the algorithm terminates and produces the final assembly.

Algorithm 1. Computation of largest *k*mer for a *de novo* transcriptome assembler with KREATION

1: **Input:** Reads $\mathcal{R}$, read length l, function f, $k_{\min}$, threshold t
2: $i = 1$
3: $k_i = k_{\min}$
4: $d\_score = 0$
5: $\mathcal{T}_{\text{previous}} = \varnothing$
6: **repeat**
7: $\quad \mathcal{T}_{k_i} = TranscriptomeAssembly(\mathcal{R}, k_i)$
8: $\quad \mathcal{C} = ComputeClusters(\mathcal{T}_{previous}, \mathcal{T}_{k_i})$
9: $\quad y_i = \log(extended(\mathcal{C}, \mathcal{T}_{k_i}))$
10: $\quad (\beta_0, \beta_1)_{i-1} = \mathrm{lm}(k_1, k_2 \ldots, k_{i-1}), (y_1, y_2 \ldots, y_{i-1}))$
11: $\quad \widehat{y}_i = \beta_0 + \beta_1 \ k_i$
12: $\quad d\_score += (y_i - \widehat{y}_i)^2$
13: $\quad$ **if** $d\_score > t$ **then**
14: $\quad\quad$ break
15: $\quad$ **else**
16: $\quad\quad \mathcal{T}_{\text{previous}} = \mathcal{T}_{\text{previous}} \cup \mathcal{T}_{k_i}$
17: $\quad\quad i = i + 1$
18: $\quad\quad k_i = f(k_{i-1})$ $\quad \triangleright$ Compute next k value
19: $\quad$ **end if**
20: **until** $k \leq l$
21: **Output:** transcripts $\mathcal{T}_{\text{previous}} \cup \mathcal{T}_{k_i}$

2.5 *De novo* removal of misassemblies

A disadvantage of merging several single *k*mer assemblies is the increased number of misassemblies in the final result. In principle, misassembled transcripts should only occur at *k*mer values that are shorter than repeat length and thus they are unlikely to occur at all different *k*mer values. To accommodate this idea we devised the following method. Assume we run our assembly for the values $k = \{k_1, k_2, k_3, k_4\}$. After producing the final clustering $\mathcal{C}$ of the transcripts of these four assemblies $\mathcal{T}_{k_1}, \mathcal{T}_{k_2}, \mathcal{T}_{k_3}, \mathcal{T}_{k_4}$ we consider the clusters c in which only transcripts of a certain $\mathcal{T}_{k_x}$ exist, i.e. which are unique with respect to $\mathcal{T}_{k_x}$. We termed these clusters as *single-k* clusters. We classified all the single-*k* clusters and transcripts shorter than a predefined length threshold (300 bp for all datasets) as misassemblies.

For measuring the difference in misassemblies between multi-*k*mer assembly (say $\mathcal{T}_{\text{multi}}$) and single-*k*mer assembly (say $\mathcal{T}_{\text{single}}$) we define:

$$\text{misassembly rate} = \frac{\text{observed}}{\text{expected}} \tag{5}$$

where,

$$\text{observed} = \frac{\#\text{misassemblies in } \mathcal{T}_{\text{multi}}}{|\mathcal{T}_{\text{multi}}|}\,, \tag{6}$$

$$\text{expected} = \frac{\#\text{misassemblies in } \mathcal{T}_{\text{single}}}{|\mathcal{T}_{\text{single}}|}\,. \tag{7}$$

2.6 Data retrieval and preprocessing

All datasets were downloaded from the SRA (http://www.ncbi.nlm.nih.gov/sra). Five RNA-seq datasets were used for analysis: 147M paired-end reads of length 50 bps for human brain (Barbosa-Morais

et al., 2012, SRR332171), 45M paired-end reads of length 45 bps for T-cell (Heap et al., 2010, SRX011545), 142M single-end reads of length 50 bps from hESCs (Au et al., 2013, SRR1020625), 64M paired-end reads of length 76 bps from HeLa cell lines (Cabili et al., 2011, SRR309265) and 60M, 101bp paired-end reads from IMR90 cell lines from ENCODE (http://genome.ucsc.edu/cgi-bin/hgFileUi?g=wgEncodeCshlLongRnaSeq).

The quality of transcriptome assembly is highly affected by the presence of sequencing errors (Le et al., 2013). Hence as a preprocessing step, all datasets were error corrected using SEECER version 0.2 (Le et al., 2013) with default parameters, except for HeLa where we used *ks*= 31 for SEECER. After each single *k*mer assembly we remove redundant transcripts in the same assembly by using CD-HIT-EST clustering (sequence identity 99%) (Fu et al., 2012) and only retaining the representative sequences of clusters.

3 Results

3.1 Common *k*mer selection strategies are suboptimal

Multi-*k*mer *de novo* transcriptome assemblers build the DBG for several *k*mer values. Conceptually, the task is to find the best multi-*k*mer assembly given a set of possible values $K = \{k_1, \ldots, k_n\}$ and a set of reads $\mathcal{R}$. There are two problems to this: (i) which metric should be used to define *optimal* performance? (ii) how to efficiently find $\widehat{K} \subseteq K$, such that $\widehat{K}$ achieves optimal performance for $\mathcal{R}$, given that there are $\sum_{i=1}^{n} \binom{n}{i}$ many such subsets?

For the first problem, one performance measure used often in the literature is the number of annotated 80%-hits in a sequence database. This is determined by aligning the transcripts to a reference sequence and comparing it with existing gene annotation, (see 'Methods'). This metric does not consider the specificity of the assembled transcripts and does not penalize for the amount of misassemblies. Here, we suggest to *optimize the sensitivity* of the multi-*k* assembly using the number of 80%-hits and use a misassembly removal strategy for the final assembly. We define the number of 80%-hits Ensembl transcripts that are obtained by running the assembler for all values in *K* for a dataset $\mathcal{R}$ as *optimal*. With this notion, we can measure the performance of any multi-*k*mer assembly with $\widehat{K} \subset K$ in terms of % *of optimal*. For example, if the exhaustive assembly using *K* produces 2000 80%-hits, we set that as optimal. If another multi-*k* assembly produces 1500 80%-hits, then it reconstructed 75% of the optimal value.

The second problem is rarely addressed in the literature, in particular the problem of selecting a subset $\widehat{K}$ given $\mathcal{R}$. In practice, the following heuristics are common: (i) use the best single *k*mer assembly according to an evaluation criteria, e.g. the one with the most BlastX hits in a close species. Here we represent this strategy by an optimistic approach selecting the single *k*mer assembly that has the highest number of known reference transcripts assembled, termed *Best-k*. (ii) Select an arbitrary subset of possible *k*mer values. We created 3 such sets for each dataset, which are called *Set 1–3* (see 'Methods'). (iii) The last strategy is to run the assembly for the full set of values in *K*. In this work we introduce KREATION (Kmer Range EstimATION), a data-driven heuristic approach which tries to maximize sensitivity without running the full set of *k*mer assemblies.

In Figure 1, we show the performance of all three previous strategies using the Oases assembler (Schulz et al., 2012) on four different human RNA-seq datasets that have different read lengths and sequencing depth (see 'Methods'). Compared to running the full set of *k*mers, which by definition is optimal, choosing a random set or picking the Best-*k* shows a loss in performance up to 30%. In particular, each setup outperforms the others on a different dataset, such that no one strategy can be recommended. KREATION achieves close to optimal performance (Fig. 1).

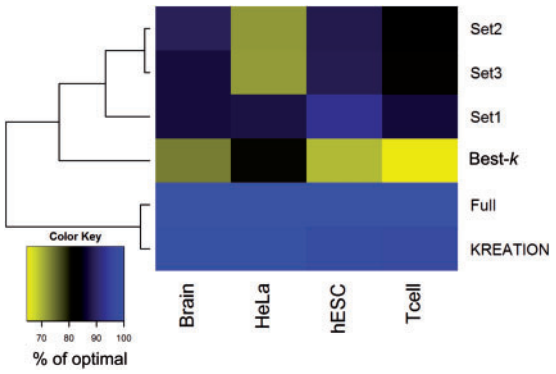

Fig. 1. Comparison of *k*mer selection strategies: random selection of a set of *k*mers (Set 1-3), best possible single *k*mer based assembly (Best-*k*), using KREATION introduced here and merging assemblies over all possible *k*mers (Full). Each column denotes one of the datasets analyzed. The intensity of the heat map encodes how many of the optimal number of 80%-hits are achieved by the approach (% of optimal)

3.2 Clustering of consecutive *k*mer assemblies reveals assembly progress

The main focus of this work is to define a data-driven procedure that predicts an optimal stopping point for a *de novo* multi-*k*mer assembler. As we mentioned earlier, we want to find a subset $\widehat{K}$ that shows a similar number of 80%-hits compared to the full assembly. First, we investigated the contribution of each single-*k*mer assembly to the performance of the full assembly using Oases. In Figure 2, we plot the number of correct transcripts that are assembled in their longest form in a particular single *k*mer assembly (x-axis). It can be seen that the assembly with the smallest *k*mer value contributes most of the correct transcripts and that a decreasing exponential trend can be observed, with higher *k*mer values being less important. From this we conclude that the problem of finding $\widehat{K}$ from all possible subsets $\sum_{i=1}^{n} \binom{n}{i}$ can be simplified. We suggest to consider a series of increasing *k*mer values $(k_1, \ldots, k_n)$, where $k_1 < k_2, \ldots, < k_n$. In this work we used the series of kmers $k_i = k_{i-1} + 2$.

In Figure 3 (bottom) it is shown how the performance (% of optimal, left y-axis) changes when the multi-*k* assembly is constructed up to index *i* in the series, i.e. $\mathcal{T}_i = \mathcal{T}_{k_1} \cup \ldots \cup \mathcal{T}_{k_i}$, by merging transcripts, (see 'Methods'). Similar to our observation in Figure 2 we see that higher *k* values contribute little to the assembly, e.g. 99% of the optimal sensitivity is reached at *k*= 39.

In a *de novo* circumstance, how can we predict the index *i* such that the obtained sensitivity is close to optimal sensitivity? We observed that the number of transcripts going from *i* to $i+1$ always increases, i.e. $|\mathcal{T}_i| > |\mathcal{T}_{i+1}|$, illustrated for a dataset in Supplementary Table 1. However, we know from Figure 2 that for higher *k* values the number of correct transcripts decreases approximately exponentially. Correct transcripts, as in Figure 2, need to be novel. These novel transcripts in $\mathcal{T}_{i+1}$ are the representative sequences of clusters that either extend transcripts in $\mathcal{T}_i$ (*extended* clusters) or form *unique* clusters, without any transcript from $\mathcal{T}_i$

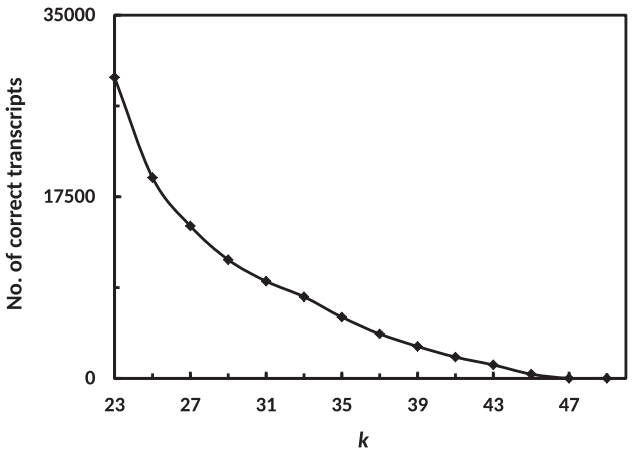

Fig. 2. Total number of correct transcripts (y-axis) which were assembled during iteration of *k*mer *k* (x-axis) in the final merged assembly. Correctness of transcripts is determined through alignment to the genome, see 'Methods' section

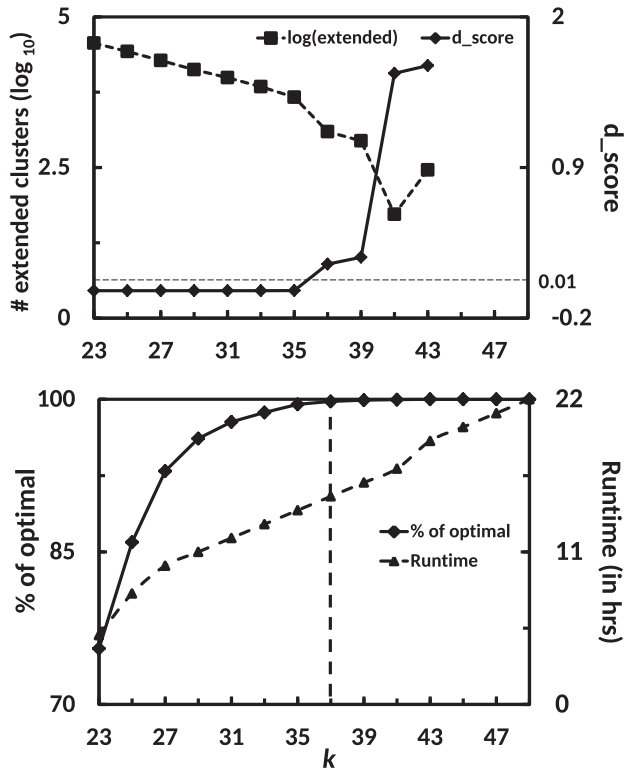

Fig. 3. Concordance between *d_score*, behaviour of extended clusters and the assembly of known transcripts. (top) The number of extended clusters (primary y-axis, log10 base) and *d_score* (secondary y-axis) is shown as a function of increasing *k* values in the multi-*k* assembly (x-axis), see text. The *d_score* crosses the threshold value (dotted horizontal line) at a *k* value after which no significant contribution is made to the assembly. This can be seen from the bottom plot which shows the contribution of each *k*mer (x-axis) towards assembly of optimal number of known 80%-hits (y-axis). The vertical dotted line represents the *k*mer where the assembly is stopped

(see 'Methods'). For KREATION we use the CD-HIT-EST algorithm that preserves sequence to cluster memberships in its output and its clustering heuristic has an added advantage of being very fast in practice.

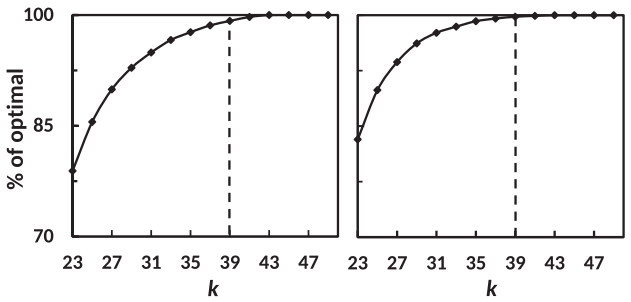

Fig. 4. Analysis of optimal *k*mer value for Trans-ABySS (left) and SOAPdenovo-Trans (right) on the brain dataset. The points in the curve represents how much of the final 80% transcripts (final here means the 80% transcript discovered using all k-values and thus termed optimal) are predicted by a multi-*k* assembly up to the current *k*mer (x-axis). The dashed line in each plot represents the optimal *k*mer suggested by KREATION

In our *de novo* setup some of the novel clusters will represent misassemblies. These misassemblies generally arise from the unique clusters (Supplementary Figure S2). Extended clusters constitute more 80%-hits than unique clusters (Supplementary Figure S3). Therefore, we can approximate the number of correct transcripts for T_{i+1} by counting extended clusters.

In Figure 3 (top) we show how the logarithm of the number of extended clusters for the brain dataset behaves for different *k* values. As the number of extended clusters also contains misassemblies we observed the exponential trend, visible as a line in log space, only up to $k = 35$. Afterwards, when fewer genuine transcripts are contributed by T_{i+1}, this trend changes. Hence, once the curve starts to deviate significantly from a straight line, dropping towards small cluster numbers, it may be advisable to stop the assembly as we do not expect contributions to the overall assembly.

3.3 Stopping the assembly by assessment of model fit

But how to measure if the exponential fit is worse after adding another *k*mer assembly?

We tested the following method. Suppose we run our assembly for values $k = k_1, k_2, \ldots, k_n$. We first fit a linear model to the log counts of extended clusters for all indices until $n - 1$, (see 'Methods'). Assuming that the predicted linear model would also explain the response variable of the current index n, we predict the log count of extended clusters for n. We then deduce the error between the actual value and the predicted value. The process is repeated for all values of n and after each iteration errors are summed up defining our *deviation score* (*d_score*). Normally the error is close to zero for data points which follow a linear trend and hence the resulting *d_score* is very small. The error becomes significantly larger at a point where the curve starts to deviate from the straight line. This results in a noticeable increase in *d_score*. As seen in Figure 3 (top), the value of *d_score* remains close to zero until $k = 37$. Namely, until a *k*mer value where all the points are well approximated by a straight line. Beyond this *k*mer the *d_score* increases significantly and goes above a pre-defined threshold (0.01 in our case). This point corresponds to a *k*mer that shows close to 99% of the optimal value (Fig. 3 bottom, dotted line). Therefore, stopping at this point results in almost no loss of assembly sensitivity and a significant reduction in runtime (Fig. 3 bottom, secondary axis). We tested this heuristics with other assemblers on the same dataset and found a similar behaviour (Fig. 4). Hence we used this heuristic to design the KREATION algorithm, see Algorithm 1.

Table 2. Analysis of assembly results with all assemblers on the five datasets

					Oases				
Dataset	kmer range	No. Transcripts	Sens. (%)	Spec. (%)	100%-hits	80%-hits	Runs saved	%hrs reduced	Runtime (hrs)
Brain	KREATION	462 896	46.59	68.98	6264	42 540	6	32	15
Brain	Full	468 056	46.74	68.94	6315	42 629	—	—	22
hESC	KREATION	196 824	37.58	73.13	12 783	42 899	8	31	9
hESC	Full	203 042	37.43	73.62	13 105	43 635	—	—	13
HeLa	KREATION	113 009	24.06	78.81	4243	25 625	15	10	162
HeLa	Full	119 009	24.1	77.43	4284	25 721	—	—	180
TCell	KREATION	129 868	19.11	77.91	3050	18 650	5	15	6
TCell	Full	132 975	19.05	75.42	3131	18 918	—	—	7
IMR90	KREATION	1 362 744	49.65	37.21	22 165	59 253	14	34	600
IMR90	Full	1 384 061	49.55	36.75	22 246	59 700	—	—	901
					SOAPdenovo-Trans				
Dataset	kmer range	No. Transcripts	Sens. (%)	Spec. (%)	100%-hits	80%-hits	Runs saved	%hrs reduced	Runtime (hrs)
Brain	KREATION	295 870	33.28	63.08	4192	25 416	5	9	11
Brain	Full	298 286	33.28	63.35	4235	25 621	—	—	12
hESC	KREATION	226 974	35.52	60.34	8072	34 914	5	25	6
hESC	Full	229 635	35.45	60.27	8128	35 087	—	—	8
HeLa	KREATION	139 955	25.63	61.89	3413	23 308	15	20	60
HeLa	Full	144 909	25.63	60.3	3456	23 559	—	—	75
TCell	KREATION	94 233	18.79	73.37	2598	16 589	4	34	4
TCell	Full	94 925	18.8	73.48	2624	16 634	—	—	6
IMR90	KREATION	1 836 920	38.58	8.65	11 936	45 276	17	10	573
IMR90	Full	1 847 582	38.99	9.71	12 720	47 308	—	—	635
					TransABySS				
Dataset	kmer range	No. Transcripts	Sens. (%)	Spec. (%)	100%-hits	80%-hits	Runs saved	%hrs reduced	Runtime (hrs)
Brain	KREATION	348 824	36.88	64.59	6715	36 531	5	10	18
Brain	Full	350 814	36.39	64.14	6766	36 629	—	—	20
hESC	KREATION	263 654	36.5	59.61	10 514	40 845	9	40	6
hESC	Full	274 615	36.72	57.95	10 975	41 618	—	—	10
HeLa	KREATION	143 423	26.8	68.56	4210	26 841	20	24	100
HeLa	Full	173 170	26.9	65.24	4402	27 460	—	—	130
TCell	KREATION	108 830	20.47	75.74	3572	212 347	4	25	4.5
TCell	Full	109 990	20.44	75.84	3608	21 409	—	—	6
IMR90	KREATION	1 396 311	44.32	19.5	18 761	57 922	23	29	560
IMR90	Full	1 470 188	46.03	22.8	20 653	60 095	—	—	780

The first row for each dataset analyses the transcripts obtained by running the assembly till the optimal *k*mer. The second row for each dataset represents the results obtained by running the assembly till a feasible *k*mer closest to the read length. KREATION used a *d_score* threshold of 0.01 for all the cases.

3.3.1 Application to other datasets

In addition to the brain dataset, we tested KREATION on four other data sets with different read length and coverage (see 'Methods'). In all cases the point where *d_score* crosses the threshold value coincides with a *k*mer value close to the optimum (see Supplementary Figure S4–S7).

We list the complete numbers for all five datasets in Table 2. As the table shows, consistently for all datasets the stopping point only leads to a small decrease in the 100 and 80%-hits. Further the final number of transcripts is reduced without affecting the nucleotide sensitivity and specificity. We also show the number of *k*mer assemblies not computed and the time saved due to KREATION. In particular, for the longer read datasets (HeLa and IMR90) KREATION avoids a significant number of assemblies, saving up to days of computation on our computing cluster. Note that the clustering done after each *k*mer assembly, only takes in the order of a few minutes as CD-HIT-EST is parallelized and very fast (Fu *et al.*, 2012).

3.3.2 Effect of d_score threshold

The threshold t for *d_score* is an important parameter for KREATION. We tested our approach for various values of t = (0.001, 0.005, 0.01, 0.05, 0.1, 0.2) on all datasets and assemblers. We found that selecting a threshold of 0.001 leads to at least a 50% reduction in runtime, and at the same time a loss up to at most 9% in comparison to the full assembly. A high threshold value results in achieving an almost 100% optimal assembly, but results in insignificant reduction of runtime (Fig. 5). For our analyses we chose a threshold value of 0.01, which seems to be a good tradeoff between runtime and quality of the final assembly, but other values may be preferred by the user.

3.4 Single-*k* clusters are enriched in misassemblies

The major drawback of a multi-*k*mer based assembly is the generation of a high number of misassemblies. We observed, and also various studies have shown, that misassemblies are generally shorter in length (see Supplementary Figure S8) and hence a large percentage of them can be removed by applying a length cutoff (300 bp in our case) on the final transcripts (Fig. 6 top). As clustering transcripts produced by different *k*mer assemblies is an integral part of KREATION, we wondered how misassemblies are distributed over the clusters. We observed that clusters which contained transcripts from only one *k*mer value consisted of a large number of misassemblies. We termed these clusters *single-k clusters* (see 'Methods'). Removing these clusters also reduces the number of misassemblies

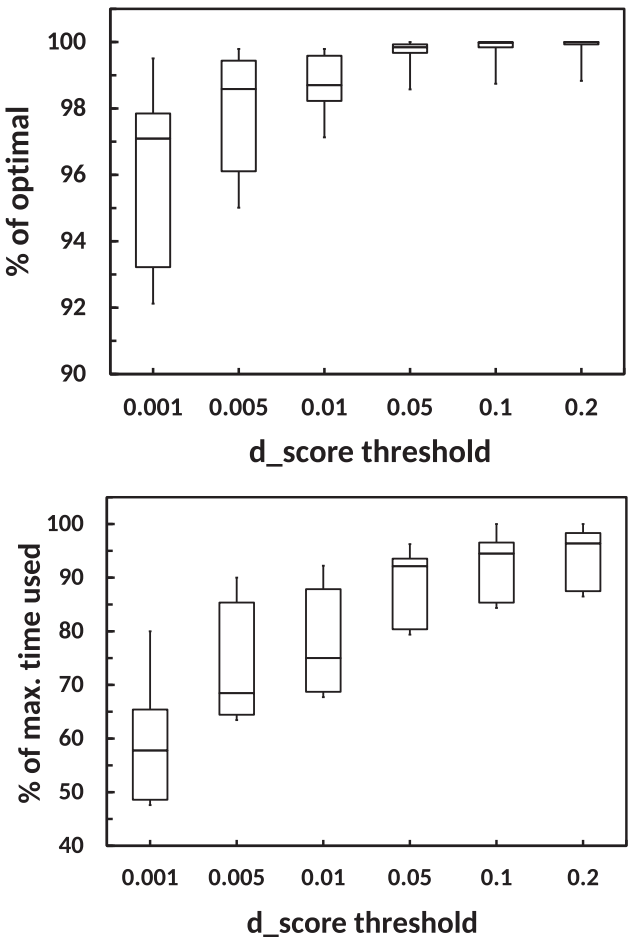

Fig. 5. Analysis of KREATION performance with different *d_score* thresholds. (top, higher is better) Assembler performance is measured as % of optimal (y-axis) for different *d_score* thresholds (x-axis). (bottom, lower is better) KREATION runtime is shown in comparison to the time taken by the Full assembly (y-axis). Each box plot shows the results for all three assemblers applied to the five data sets

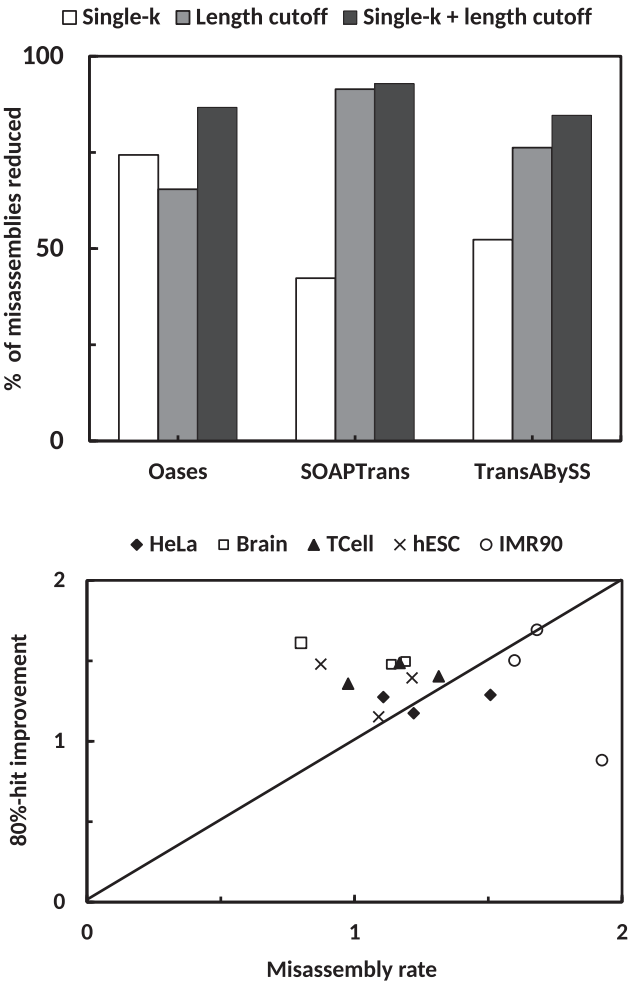

Fig. 6. Analysis of different misassembly removal strategies. (top) The bar plot represents the performance of various removal strategy in terms of percentage of misassemblies removed on Brain dataset. Single-*k* cluster removal (white bar) and 300 bp length cutoff based removal (grey bar) removes a high percentage of misassemblies. A combination of both methods (black bar) performs better than applying only one strategy. (bottom) Comparison of 80%-hit improvement rate and misassembly rate for all computed assemblies (see 'Methods')

significantly (Fig. 6 top). We found that removing all transcripts which are either shorter than the length cutoff or which belong to single-*k* clusters reduces more misassemblies as compared to applying only one of the above mentioned filters (Fig. 6 top).

Further we wanted to check whether merging assemblies from multiple *k*mer values as done in KREATION is better than the single-*k*mer assembly with the highest sensitivity (k_1 in our case). In other words, we wanted to check whether we are generating more misassemblies than useful transcripts, when we merge assemblies from multiple *k*mer values. For this, we define *80%-hit improvement rate* as the fold-change of 80%-hits from the assembly generated by the lowest *k*mer and *misassembly rate* as the ratio of observed to the expected number of misassemblies. Figure 6 (bottom) shows the comparison between these two metrics for all KREATION assemblies computed, separated by dataset. In an ideal situation, the 80%-hit improvement rate should be better than the misassembly rate and hence all the points in the graph should be above the diagonal. We show that for most of the datasets the corresponding points are either above the diagonal or close to the diagonal, except for the HeLa dataset assembled by TransABySS, which has a misassembly rate of 1.93. We conclude that the multi-*k*mer based assembly approach followed by appropriate filtering of misassemblies is better than the single *k*mer based assembly.

4 Discussion and conclusion

We have presented KREATION, an algorithm that is able to automatically stop a *de novo* multi-*k* transcriptome assembly at a *k*mer value close to the optimal sensitivity. We showed that clustering newly assembled transcripts with all assemblies made in previous rounds can be used to estimate how many transcripts have been improved due to the last round, by counting extended clusters. We empirically found that the number of extended clusters falls exponentially with increasing *k*, when we consider to run the multi-*k* assembler from smaller *k*mer values to larger ones, as is most reasonable for transcriptome assemblies. This motivated us to predict the *k*mer value at which the assembly should stop by selecting the *k*mer where deviation to the expected exponential trend deviates considerably, as measured with the designed the *d_score*. We have shown that thresholding the *d_score* works well for three popular *de novo* assemblers, and datasets with different coverages and read lengths. For longer read datasets KREATION may save days of computation.

However, KREATION is a heuristic approach and there is no guarantee that the *d_score* threshold corresponds to a good stopping point or that there will be an optimum for the set of *k*mers tested, albeit both is true for the datasets and assemblers tested in this work. Still, we think that there is a theoretical connection that is worth exploring further. KREATION often selects different stopping *k*mer values for each assembler when applied to the same dataset. This points to a complex interplay between graph structure, transcriptome complexity, read coverage and assembler implementations. It may be the reason why simpler strategies for selecting *k*mers do not seem to generalize for datasets with different characteristics (*cf*. Fig. 1).

One disadvantage of merging the assemblies of several *k* values is the increased number of misassemblies as compared to using one kmer. However, recent studies have shown that appropriate filters (Yang and Smith, 2013) or a proper statistical treatment with replicate data (Davidson and Oshlack, 2014) allows to remove most misassemblies and therefore ease downstream analyses. Here we show that a large number of misassemblies stem from single-*k* clusters that can be removed easily. Together with a length cutoff on assembled transcripts this denotes a powerful approach to get rid of most of the misassemblies without removing genuine transcripts (Fig. 6, Supplementary Figure S9). We argue that this makes multi-*k*mer assembly strategies more useful for the community, but we think that there is still room for improvement for removing misassemblies.

In a recent work (Li *et al*., 2014) a reference free transcriptome assembly evaluation approach was introduced. Based on a graphical model of the RNA-sequencing process, an assembly quality estimate can be computed by aligning reads to the assembled transcripts. We note that in principle their method may be used as an alternative function to decide when to stop. However, this approach would constitute a serious runtime cost as read alignment, SAM file writing and model building would take in the order of hours for one *k*mer iteration. Instead, we see their work complementary to our work. We have focused on the question where to stop the assembly, but there are other parameters that are worth tuning. For example, we are currently assuming the k_1 is given, which is partly due to the fact that it just needs to be chosen in such a way to avoid small *k*mers that produce misassemblies.

As a conclusion, we show that an informed *k*mer selection approach for *de novo* transcriptome assembly shows an improvement over simpler methods suggested so far. We believe that KREATION with the misassembly filters will be useful for the community and implemented the mentioned ideas in a software that currently supports the *de novo* assemblers tested in this work (https://github.com/SchulzLab/KREATION).

Acknowledgement

We like to thank the anonymous reviewers for their constructive comments.

Funding

This work was supported by the Cluster of Excellence on Multimodal Computing and Interaction (EXC284) of the German National Science Foundation (DFG).

References

Au,K.F. *et al*. (2013) Characterization of the human ESC transcriptome by hybrid sequencing. *Proc.Natl. Acad. Sci. USA*, **110**, E4821–E4830.

Barbosa-Morais,N.L. *et al*. (2012) The evolutionary landscape of alternative splicing in vertebrate species. *Science*, **338**, 1587–1593.

Cabili,M.N. *et al*. (2011) Integrative annotation of human large intergenic noncoding RNAs reveals global properties and specific subclasses. *Genes Dev*., **25**, 1915–1927.

Chang,Z. *et al*. (2015) Bridger: a new framework for de novo transcriptome assembly using rna-seq data. *Genome Biol*., **16**, 30. Zheng Chang and Guojun Li contributed equally to this work.

Chikhi,R. and Medvedev,P. (2014) Informed and automated k-mer size selection for genome assembly. *Bioinformatics*, **30**, 31–37.

Cunningham,F. *et al*. (2014) Ensembl 2015. *Nucleic Acids Res*., **43**, D662–D669.

Davidson,N.M. and Oshlack,A. (2014) Corset: enabling differential gene expression analysis for de novo assembled transcriptomes. *Genome Biol*., **15**, 410.

Fu,L. *et al*. (2012) CD-HIT: accelerated for clustering the next-generation sequencing data. *Bioinformatics*, **28**, 3150–3152.

Grabherr,M.G. *et al*. (2011) Full-length transcriptome assembly from RNA-Seq data without a reference genome. *Nat. Biotechnol*., **29**, 644–652.

Haznedaroglu,B.Z. *et al*. (2012) Optimization of de novo transcriptome assembly from high-throughput short read sequencing data improves functional annotation for non-model organisms. *BMC Bioinformatics*, **13**, 170.

Heap,G.A. *et al*. (2010) Genome-wide analysis of allelic expression imbalance in human primary cells by high-throughput transcriptome resequencing. *Hum. Mol. Genet*., **19**, 122–134.

Ilie,L. *et al*. (2011) HiTEC: accurate error correction in high-throughput sequencing data. *Bioinformatics*, **27**, 295–302.

Kent,W.J. (2002) BLAT—The BLAST-Like alignment tool. *Genome Res*., **12**, 656–664.

Le,H.S. *et al*. (2013) Probabilistic error correction for RNA sequencing. *Nucleic Acids Res*., **41**, e109.

Li,B. *et al*. (2014) Evaluation of de novo transcriptome assemblies from RNA-Seq data. *Genome Biol*., **15**, 553.

Peng,Y. *et al*. (2013) IDBA-tran: a more robust de novo de Bruijn graph assembler for transcriptomes with uneven expression levels. *Bioinformatics*, **29**, i326–i334.

Robertson,G. *et al*. (2010) De novo assembly and analysis of RNA-seq data. *Nat. Methods*, **7**, 909–912.

Schulz,M.H. *et al*. (2012) Oases: robust de novo RNA-seq assembly across the dynamic range of expression levels. *Bioinformatics*, **28**, 1086–1092.

Schulz,M.H. *et al*. (2014) Fiona: a parallel and automatic strategy for read error correction. *Bioinformatics*, **30**, i356–i363.

Simpson,J.T. (2014) Exploring genome characteristics and sequence quality without a reference. *Bioinformatics*, **30**, 1228–1235.

Sloan,D.B. *et al*. (2012) De novo transcriptome assembly and polymorphism detection in the flowering plant Silene vulgaris (Caryophyllaceae). *Mol. Ecol. Resour*., **12**, 333–343.

Sultan,M. *et al*. (2008) A global view of gene activity and alternative splicing by deep sequencing of the human transcriptome. *Science*, **321**, 956–960.

Surget-Groba,Y. and Montoya-Burgos,J.I. (2010) Optimization of de novo transcriptome assembly from next-generation sequencing data. *Genome Res*., **20**, 1432–1440.

Xie,Y. *et al*. (2014) SOAPdenovo-Trans: de novo transcriptome assembly with short RNA-Seq reads. *Bioinformatics*, **30**, 1660–1666.

Yang,Y. and Smith,S.A. (2013) Optimizing de novo assembly of short-read RNA-seq data for phylogenomics. *BMC Genomics*, **14**, 328.